

## ORIGINAL ARTICLE

# Cisplatin resistance and malignant behaviors of lung cancer cells are promoted by circ\_0002360 via targeting miR-6751-3p to regulate the expression of ZNF300

Lingyan Ding<sup>1</sup> | Lizhi Li<sup>2</sup> | Zhaohui Tang<sup>1</sup> 

<sup>1</sup>Department of Oncology, The Central Hospital of Yongzhou, Yongzhou City, China

<sup>2</sup>Department of Ultrasonography, The Central Hospital of Yongzhou, Yongzhou City, China

## Correspondence

Zhaohui Tang, Department of Oncology, The Central Hospital of Yongzhou, No. 396, Yiyun Road, Lengshuitan District, Yongzhou City, Hunan Province 425100, China.  
Email: peiyong20102020@163.com

## Abstract

**Background:** Circular RNAs (circRNAs) are key regulators in oncogenesis and chemoresistance of human cancers. Herein, we focused on the roles of circ\_0002360 in regulating lung cancer progression and cisplatin (DDP) resistance.

**Methods:** The detection of circ\_0002360, microRNA-6751-3p (miR-6751-3p) and zinc finger protein 300 (ZNF300) was conducted via reverse transcription-quantitative polymerase chain reaction assay. Cell sensitivity was determined using cell counting kit-8 assay. Proliferation detection was performed by colony formation assay and EdU assay. The migrated cells were examined via transwell assay. Cell apoptosis analysis was carried out through flow cytometry and caspase 3 activity assay. Western blot was used to examine the protein levels. Target interaction was confirmed through dual-luciferase reporter assay and RNA immunoprecipitation assay. Circ\_0002360 function in vivo was performed via xenograft tumor assay.

**Results:** Circ\_0002360 was overexpressed in DDP-resistant lung cancer tissues and cells. Silencing circ\_0002360 inhibited DDP resistance, proliferation and migration but enhanced apoptosis of DDP-resistant cells. Circ\_0002360 could elevate ZNF300 expression. DDP resistance and lung cancer progression were also impeded by ZNF300 down-regulation. ZNF300 overexpression reversed the function of circ\_0002360 knockdown in DDP-resistant lung cancer cells. The regulation of circ\_0002360 for ZNF300 was achieved by sponging miR-6751-3p. Circ\_0002360 promoted DDP resistance in xenograft mice through mediating the miR-6751-3p/ZNF300 axis.

**Conclusion:** Circ\_0002360 targeted miR-6751-3p to regulate ZNF300 level, thus elevating DDP resistance and promoting the malignant progression of lung cancer cells.

## KEYWORDS

circ\_0002360, cisplatin resistance, lung cancer, miR-6751-3p, ZNF300

## INTRODUCTION

Lung cancer is a common type of cancer worldwide, with an estimated 2 million new cases and 1.76 million death cases each year.<sup>1</sup> Chemotherapy remains the central treatment strategy for lung cancer at different stages, but cancer cells are inclined to become resistant to therapeutic drugs.<sup>2</sup> Cisplatin (DDP) is a platinum-based chemotherapy which acts as a first-line treatment drug for lung cancer patients.<sup>3</sup> Nevertheless, its clinical application has been limited by drug

resistance and other remedial countermeasures are therefore necessary.<sup>4</sup>

Non-coding RNAs (ncRNAs) are associated with chemoresistance in various kinds of human cancers, including lung cancer.<sup>5</sup> The closed-loop circular RNAs (circRNAs) can lead to gene level changes through functioning as molecular sponges for small microRNAs (miRNAs), thus inducing the regulation of cancer biology and tumor resistance.<sup>6-8</sup> For instance, Xu et al. showed that circ\_0002874/miR-1273f/MDM2 regulated paclitaxel resistance

in lung cancer.<sup>9</sup> Zhu et al. stated that circRNA\_103809 promoted the resistance to DDP of lung cancer cells via miR-377-3p-mediated GOT1 alteration.<sup>10</sup>

Hsa\_circ\_0002360 (circ\_0002360) has been indicated to be highly expressed and play a key role in tongue squamous cell carcinoma.<sup>11</sup> In addition, circ\_0002360 was found to be upregulated and implicated in the progression of lung adenocarcinoma via miR-3620-5p/PHF19 pathway.<sup>12</sup> However, the effect of circ\_0002360 on chemoresistance of lung cancer remains unclear. Zinc finger protein 300 (ZNF300) is a typical zinc finger protein with promoting effects on aggressive behaviors and DDP resistance in lung cancer cells.<sup>13</sup> MicroRNA-6751 (miR-6751) was revealed to elevate chemosensitivity in DDP-resistant ovarian cancer cell lines.<sup>14</sup> The involvement of miR-6751-3p in lung cancer is unknown. Moreover, the association among circ\_0002360, miR-6751-3p and ZNF300 in regulating DDP resistance requires further research.

Herein, circ\_0002360 was hypothesized to regulate ZNF300 expression through miR-6751-3p sponging effect. The purpose of this study was to investigate the regulatory mechanism of circ\_0002360 in lung cancer progression and DDP resistance.

## METHODS

### Patient samples

A total of 50 paired tumor tissues and normal controls (NC) were collected from lung cancer patients ( $n = 50$ ) of the Central Hospital of Yongzhou. A total of 27 patients with DDP therapy had recurrent disease, and tumor tissues were considered as the DDP-resistant (Tumor-R) group. Twenty-three patients had not received any therapy, and tumor tissues were considered as the DDP-sensitive (Tumor-S) group. This study was performed based on the informed consent of these patients and permitted by the Ethics Committee of the Central Hospital of Yongzhou.

**TABLE 1** Primer sequences used for RT-qPCR

Name	Primers for PCR (5'-3')	
hsa_circ_0002360	Forward	CACTCCACTGCCTTTAACCCCT
	Reverse	GGGCCCATCCACTGTGATTTT
ZNF300	Forward	TGTGACAGCGGTTCCCATTA
	Reverse	CCATGTGGAGGAGGGATCAT
miR-6751-3p	Forward	GCCGAGACTGAGCCTCTCTCT
	Reverse	CTCAACTGGTGTCTGGGAGT
RUNX1	Forward	GGAAGTCAACCTCTGCTGCT
	Reverse	TCGGACCACAGAGCACTTTC
GAPDH	Forward	GACAGTCAGCCGCATCTTCT
	Reverse	GCGCCCAATACGACCAAATC
U6	Forward	CTCGCTTCGGCAGCACA
	Reverse	AACGCTTCACGAATTTGCGT

## Cell culture and transfection

Lung cancer cells (A549, H1299) and chemoresistant cells (A549/DDP, H1299/DDP) were provided by BioVector NTCC Inc. Dulbecco's modified Eagle medium (DMEM; Gibco) with a complement of 10% fetal bovine serum (FBS; Gibco) and 1% antibiotics (Gibco) was prepared. Then, 10  $\mu\text{g/ml}$  DDP (Sigma) was added to the culture media of resistant cells to maintain drug resistance. Cells were cultured with the mixed solution in 5%  $\text{CO}_2$  at 37°C.

Lentiviral vectors of short hairpin RNAs (shRNAs) targeting circ\_0002360 or ZNF300 (sh-circ\_0002360, sh-ZNF300) and shRNA control vector (sh-NC) were synthesized by Ribobio. ZNF300 sequence was inserted into the pcDNA vector (Invitrogen) to construct the pcDNA-ZNF300 vector (ZNF300). The mimic and inhibitors for miR-6751-3p or miRNA controls (miR-6751-3p, anti-miR-6751-3p, miR-NC, anti-NC) were purchased from Ribobio. Then, 70% confluent DDP-resistant cells were conducted with transfection of these vectors or RNAs using lipofectamine 3000 (Invitrogen).

## Reverse transcription-quantitative polymerase chain reaction (RT-qPCR) assay

The collected tissues and cells were lysed for RNA extraction using TRI reagent (Sigma), then reverse transcription for complementary DNA (cDNA) was performed via a QuantiTect reverse transcription kit (Qiagen). The amplified reaction was completed by QuantiTect SYBR green PCR kit (Qiagen) as per the manufacturer's guidelines. Data calculation was conducted by the  $2^{-\Delta\Delta\text{Ct}}$  method,<sup>15</sup> and glyceraldehyde-phosphate dehydrogenase (GAPDH) or U6 was applied for level normalization. The sequences of all primers are shown in Table 1. In addition, RNA was isolated from the nucleus and cytoplasm via PARI Kit (Invitrogen). The levels of circ\_0002360, U6 and GAPDH were then detected through RT-qPCR.

## Cell counting kit-8 (CCK-8) assay

The cells were treated with DDP for 24 h, followed by incubation in a 10  $\mu\text{l/well}$  CCK-8 solution (Beyotime). After 2 h, absorbance in a microplate reader was measured at 450 nm. Half inhibitory concentration (IC50) was defined as the concentration of DDP at 50% cell viability.

## Colony formation assay

We then seeded 12-well plates with 200 transfected cells/well. After culture for 14 days, 0.1% crystal violet (Sigma) was exploited for colony staining at 25°C, and 15 min later, the stained colonies were counted using Image J software (NIH).

## EdU assay

At 24 h post-transfection, proliferation capacity was examined via an EdU imaging detection kit (KeyGEN). Cells were labeled with EdU solution and nuclei were stained with diamidine phenylindole (DAPI; Sigma), followed by image acquisition via a fluorescence microscope (Olympus). EdU incorporation was expressed as the percentage of EdU and DAPI merged cells.

## Transwell assay

The Transwell chamber (Corning Inc.) was inoculated with  $1 \times 10^4$  cells and 500  $\mu$ l medium in the upper and lower chambers, respectively. After the chamber was incubated for 24 h, the migrated cells in the bottom were colored with 0.1% crystal violet (Sigma) and counted using an inverted microscope (Olympus). The images were saved at 100 $\times$  magnification.

## Flow cytometry

Annexin V Apoptosis Kit (Beyotime) was exploited for apoptosis analysis of transfected cells. Then, 200  $\mu$ l binding

buffer was employed to resuspend cells, followed by staining of  $2 \times 10^5$  cells with 10  $\mu$ l Annexin V-fluorescein isothiocyanate (FITC) and propidium iodide (PI). Twenty minutes later, apoptotic cells were observed under the flow cytometer (BD Biosciences). Cell apoptosis rate was indicated by apoptotic cells/total cells  $\times$  100%.

## Caspase 3 activity assay

Cell apoptosis was further evaluated by Caspase 3 activity assay kit (Beyotime). Transfected cells were lysed in 100  $\mu$ l lysis buffer for 15 min on the ice, then centrifuged with 15 000 $\times g$  at 4 $^{\circ}$ C for 10 min. Then, cell supernatant was transferred for caspase 3 activity detection according to the manufacturer's instructions.

## Western blot

Whole cell lysis assay kit (KeyGen) and BCA protein assay kit (KeyGen) were employed for extraction of total proteins and detection of protein concentration, respectively. Protein examination was carried out as previously stated.<sup>16</sup> The antibodies including antimultidrug resistance associated protein 1 (anti-MRP1; Abcam, ab230948, 1:1000),

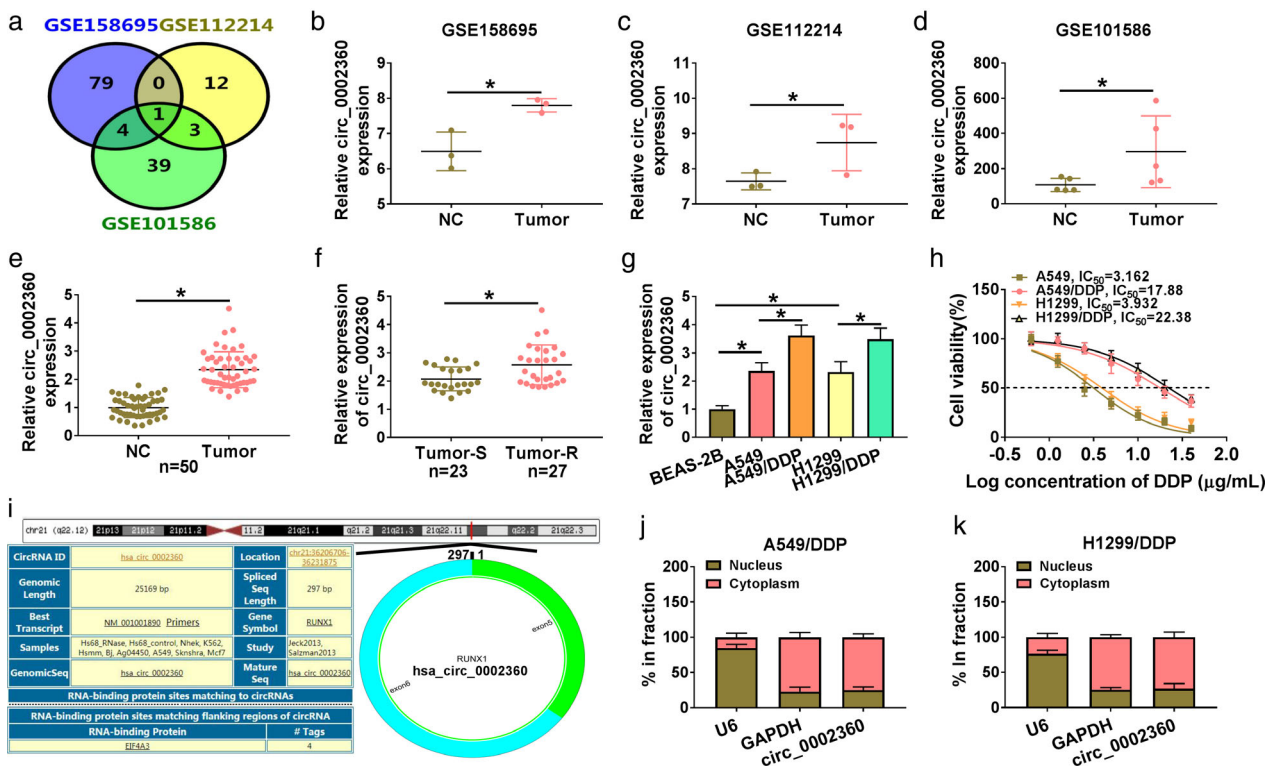


**FIGURE 1** Upregulation of circ\_0002360 in DDP-resistant lung cancer samples and cells. (a) The dysregulated circRNA was screened by online datasets. (b–d) The expression level of circ\_0002360 in GSE158695, GSE112214 and GSE101586. (e,f) Circ\_0002360 was quantified by RT-qPCR in lung cancer samples (e) and DDP-resistant samples (f). (g) The level of circ\_0002360 was detected by RT-qPCR in A549, A549/DDP, H1299, and H1299/DDP cells. (h) IC<sub>50</sub> of DDP was determined by CCK-8 assay in parental and DDP-resistant lung cancer cells. (i) The genic information of circ\_0002360. (j,k) The localization of circ\_0002360 was analyzed by RT-qPCR in cytoplasm and nucleus of A549/DDP and H1299/DDP cells. \**p* < 0.05

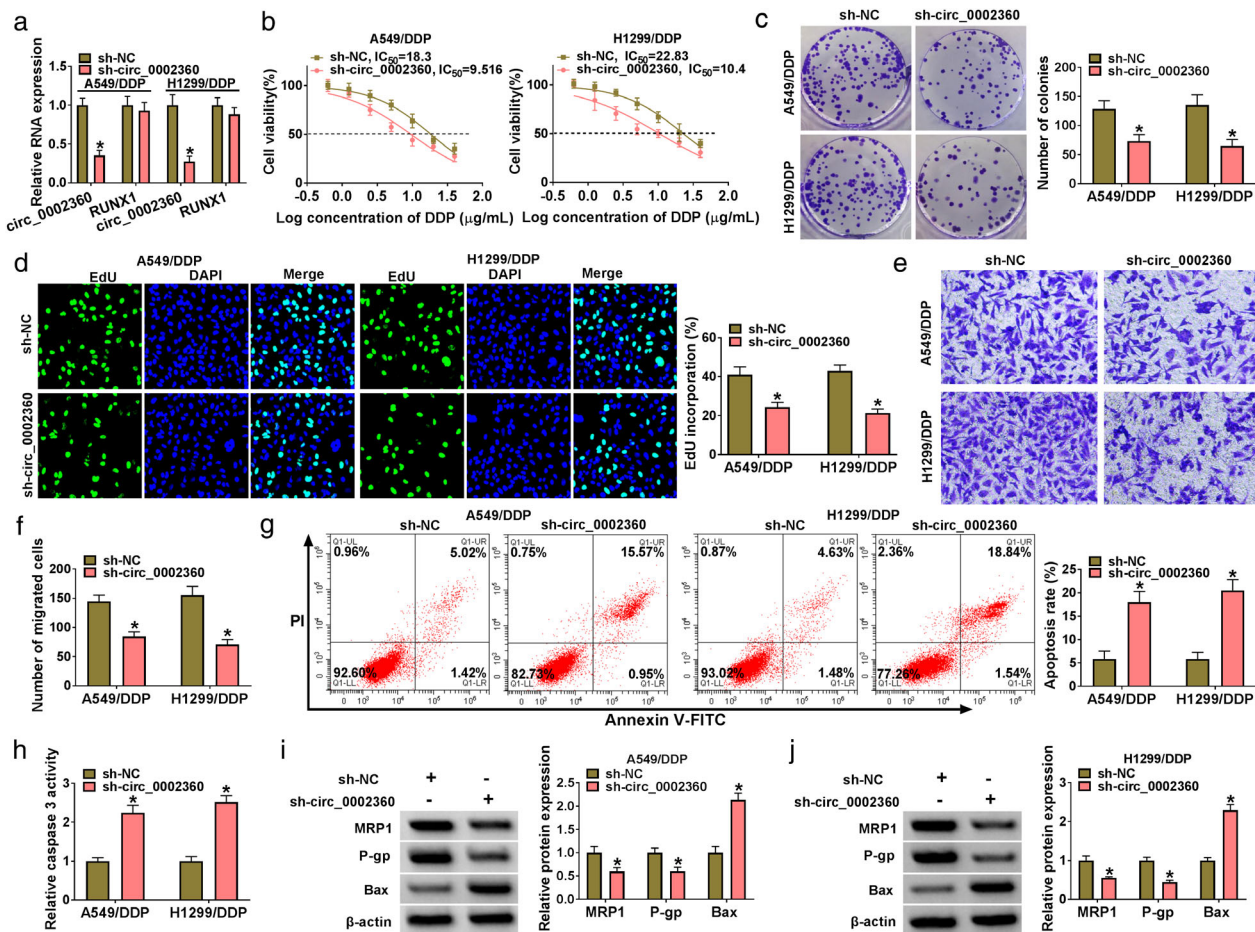


**FIGURE 2** Silencing circ\_0002360 reduced DDP resistance and suppressed malignant phenotypes of DDP-resistant lung cancer cells. A549/DDP and H1299/DDP cells were transfected with sh-NC or sh-circ\_0002360. (a) RT-qPCR was applied to determine the circ\_0002360 and RUNX1 levels. (b) A CCK-8 assay examined IC<sub>50</sub> of DDP. (c,d) Colony formation assay (c) and EdU assay (d) were applied to analyze cell proliferation. (e) Transwell assay was applied to evaluate cell migration. (g,h) Flow cytometry (g) and caspase 3 activity (h) were applied to assess cell apoptosis. (i,j) Western blot was applied to measure the protein levels of MRP1, P-gp and Bax. \**p* < 0.05

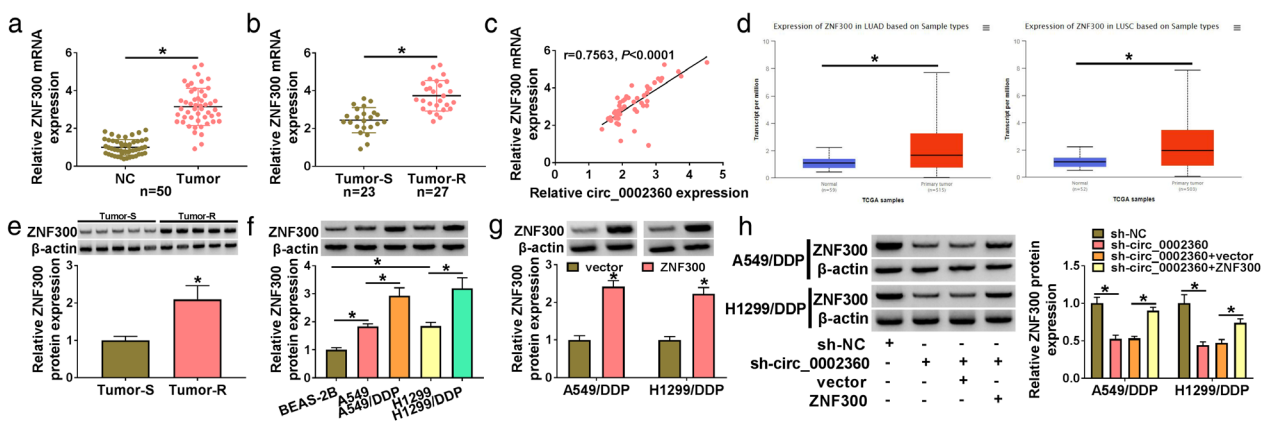


**FIGURE 3** Circ\_0002360 positively regulated the level of ZNF300. (a–b) ZNF300 mRNA expression was assayed using RT-qPCR in lung cancer tissues (a) and tumor-R tissues (b). (c) The linear relation between circ\_0002360 and ZNF300 was analyzed using Pearson's correlation coefficient. (d) TCGA data showed the upregulation of ZNF300 in LUAD and LUSC. (e,f) ZNF300 protein level was determined by western blot in tumor-S and tumor-R samples (e), as well as in parental and resistant lung cancer cells (f). (g) Transfection efficiency of ZNF300 was assessed by western blot in A549/DDP and H1299/DDP cells. (h) Western blot was used for protein analysis of ZNF300 in sh-NC, sh-circ\_0002360, sh-circ\_0002360 + vector and sh-circ\_0002360 + ZNF300 groups. \**p* < 0.05

anti-P-glycoprotein P (anti-p-gp; Abcam, ab170904, 1:1000), anti-Bcl-2 associated  $\times$  (anti-Bax; Abcam, ab182733, 1:1000), anti-ZNF300 (Abcam, ab202965, 1:1000), anti- $\beta$ -actin (Abcam, ab8227, 1:1000), anti-rabbit IgG, HRP-linked antibody (Abcam, ab205718, 1:5000) were examined. The blots were visualized by ECL Substrate Kit (Abcam), followed by protein analysis via Image J software (NIH).

## Dual-luciferase reporter assay

The pmirGLO plasmid (Promega) was cloned with wild-type (WT) circ\_0002360 and ZNF300 3'UTR sequences to generate WT-circ\_0002360 and WT-ZNF300 3'UTR. The mutant-type (MUT) plasmids MUT-circ\_0002360 and MUT-ZNF300 3'UTR were constructed as the negative controls. The cotransfection of luciferase plasmid and miR-NC or miR-6751-3p was performed for 48 h, then A549/DDP and H1299/DDP cells were harvested for luciferase intensity analysis using dual-luciferase reporter detection kit (Promega).

## RNA immunoprecipitation (RIP) assay

The interaction between targets was validated via Magna RIP RNA-binding protein immunoprecipitation kit (Millipore) following the provided guidelines. Anti-immunoglobulin G (anti-IgG) served as the negative control for anti-argonaute-2 (anti-Ago2). The magnetic beads were washed and total RNA was extracted for gene expression detection via RT-qPCR.

## Tumor xenograft assay

BALB/c male nude mice were subcutaneously injected with  $1 \times 10^6$  sh-NC or sh-circ\_0002360 transfected H1299/DDP and A549/DDP cells, with six mice in each group. Mice were subsequently treated with 2 mg/kg DDP every two days. Tumor volume was determined weekly using the formula: length  $\times$  width<sup>2</sup>  $\times$  0.5, then tumors were dissected from the euthanized mice after 28 days. RNA or protein level detection was carried out through RT-qPCR and western blot.

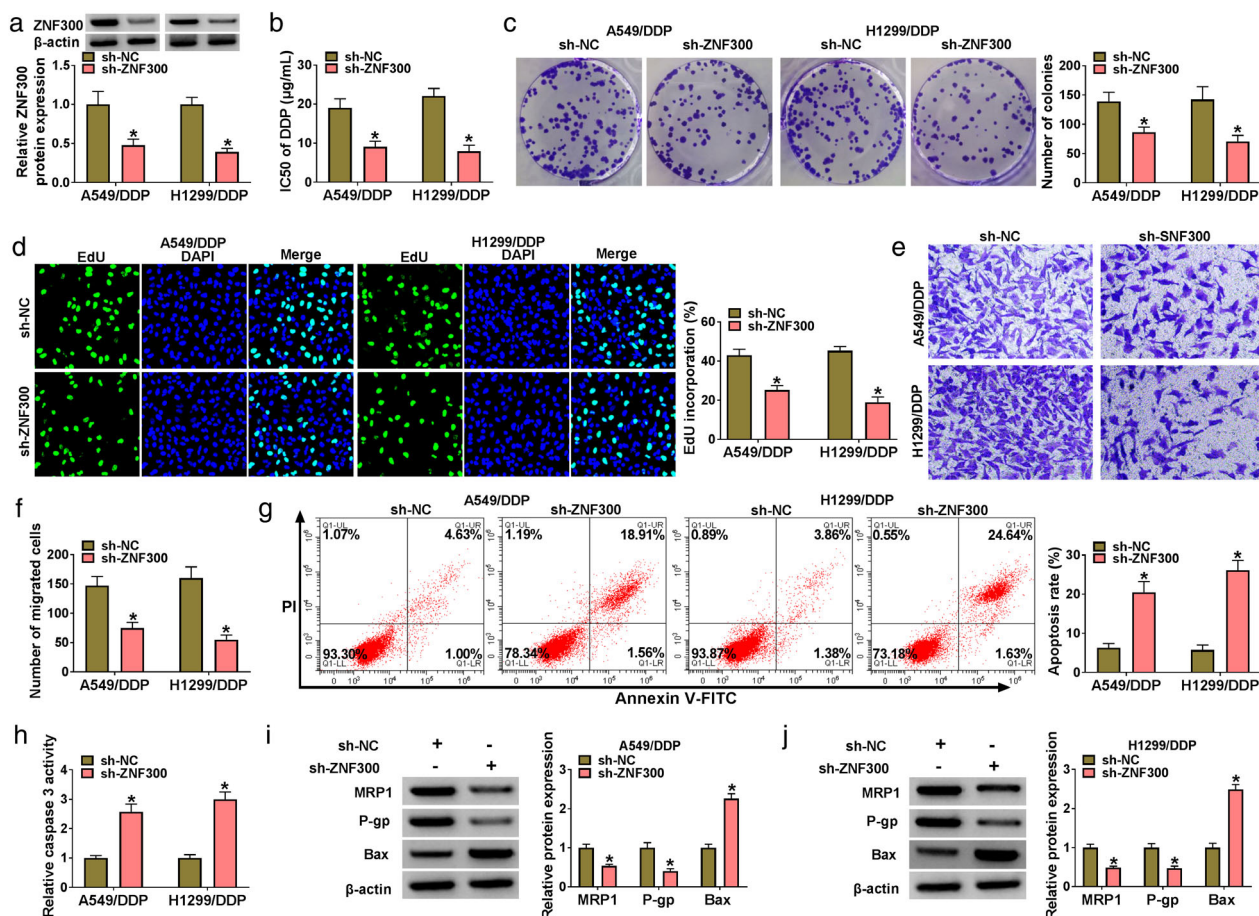


**FIGURE 4** ZNF300 downregulation inhibited DDP resistance and lung cancer progression. A549/DDP and H1299/DDP cells were performed with transfection of sh-NC or sh-ZNF300. (a) RT-qPCR was conducted for ZNF300 protein detection. (b) CCK-8 assay was conducted for measuring the IC<sub>50</sub> of DDP. (c,d) Colony formation assay (c) and EdU assay (d) were conducted for proliferation examination. (e) Transwell assay was conducted for assessment of migration. (g,h) Flow cytometry (g) and caspase 3 activity (h) were conducted for determination of apoptosis. (i,j) Western blot was conducted for protein analysis of MRP1, P-gp and Bax. \**p* < 0.05

The protein levels of Ki67 (Abcam, ab15580) and ZNF300 (Abcam, ab202965) were examined via immunohistochemistry (IHC) assay.<sup>17</sup> In addition, tumor growth was monitored in a xenograft model of H1299 + PBS, H1299 + DDP, H1299/DDP + PBS and H1299/DDP + DDP groups, as well as A549 + PBS, A549 + DDP, A549/DDP + PBS and A549/DDP + DDP groups. The mice were provided by Vital River Laboratory Animal Technology Co., Ltd. The protocols were authorized by the Animal Ethical Committee of the Central Hospital of Yongzhou.

## Statistical analysis

Three replicates were carried out in the experiments of this study. The relationship was analyzed via Pearson's correlation coefficient. Data were revealed as the mean  $\pm$  standard deviation, followed by data analysis using SPSS 22.0 (SPSS Inc.). Through the analysis of Student's *t*-test and analysis of variance (ANOVA) followed by Tukey's test, the significant difference ( $p < 0.05$ ) was evaluated.

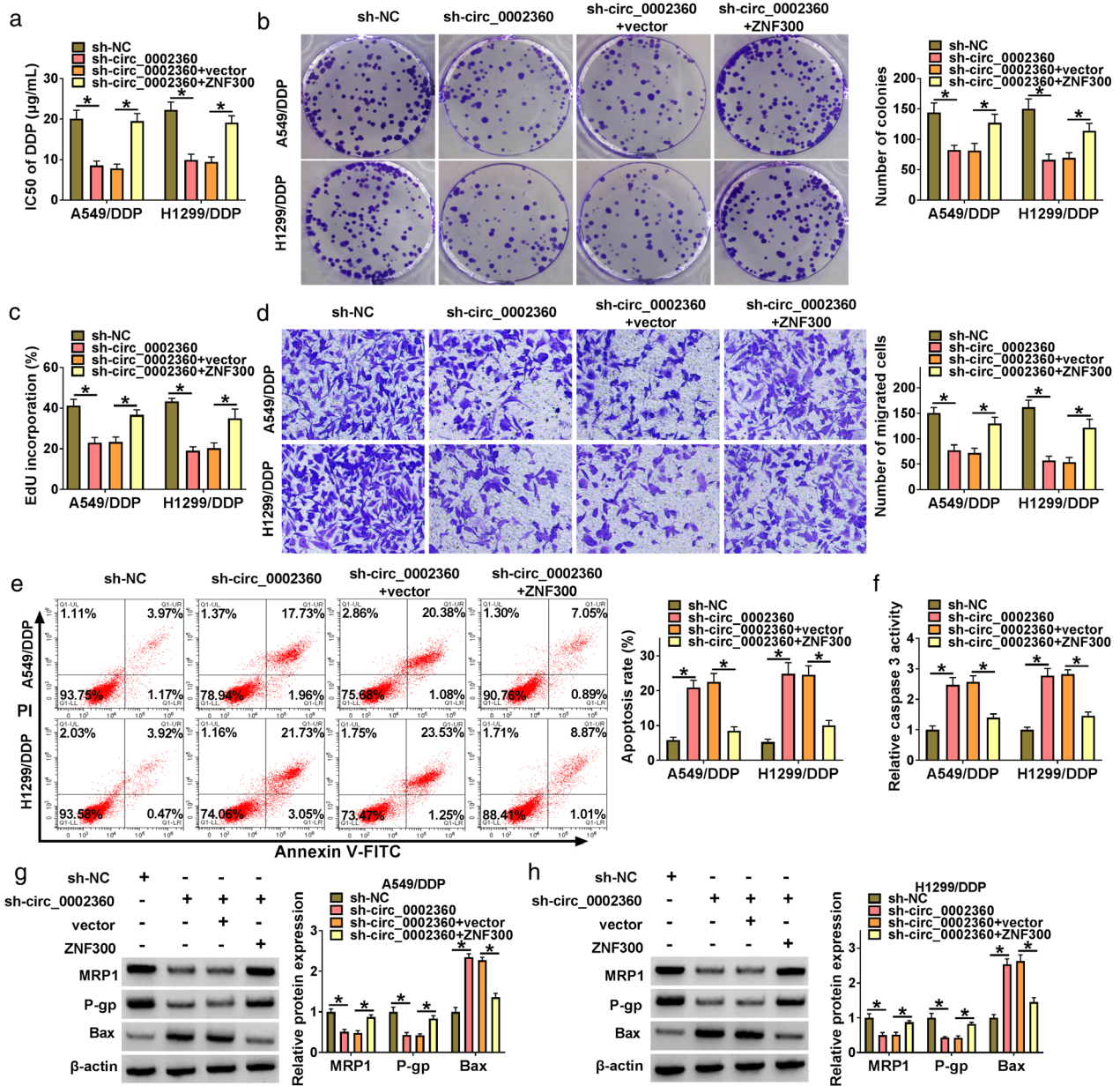


**FIGURE 5** Circ\_0002360 acted in DDP-resistant lung cancer cells via upregulating ZNF300. Transfection of sh-NC, sh-circ\_0002360, sh-circ\_0002360 + vector and sh-circ\_0002360 + ZNF300 was performed in A549/DDP and H1299/DDP cells. (a) IC<sub>50</sub> of DDP was determined through CCK-8 assay. (b,c) The proliferation ability was examined through colony formation assay (b) and EdU assay (c). (d) The migration potential was analyzed through transwell assay. (e,f) Cell apoptosis was assessed through flow cytometry (e) and caspase 3 activity (f). (g,h) MRP1, P-gp and Bax levels were detected through western blot. \* $p < 0.05$

## RESULTS

## Upregulation of circ\_0002360 in DDP-resistant lung cancer samples and cells

The dysregulated circRNAs were screened through the online datasets. Circ\_0002360 is a mutual circRNA from GSE158695, GSE112214 and GSE101586 (Figure 1a). Three datasets showed that the expression level of circ\_0002360 was markedly increased in lung cancer tissues relative to the normal controls (Figure 1b–d). Also, the upregulation of circ\_0002360 in 50 lung cancer samples relative to the normal samples (Figure 1e) was detected. In addition, circ\_0002360 expression was higher in tumor-R tissues compared with tumor-S tissues (Figure 1f). Circ\_0002360 was also upregulated in A549 and H1299 cells contrasted to BEAS-2B cells, as well as in A549/DDP and H1299/DDP cells contrasted to A549 and H1299 cells (Figure 1g). IC50 of DDP has been indicated to be elevated in A549/DDP and H1299/DDP cells compared to that in A549 and H1299 cells, suggesting the DDP resistance in A549/DDP and H1299/DDP cells (Figure 1h). Circ\_0002360 is produced from exon5 and exon 6 of RUNX family transcription factor 1 (RUNX1) with spliced sequence length of 297 bp (Figure 1i). By comparison with the distribution of U6 and GAPDH in nucleus and cytoplasm, circ\_0002360 was affirmed to be localized in the cytoplasm of A549/DDP and H1299/DDP cells (Figure 1j,k). All these data implied that circ\_0002360 might be an important regulator in DDP-resistant lung cancer.

## Silencing circ\_0002360 reduced DDP resistance and suppressed malignant phenotypes of DDP-resistant lung cancer cells

Transfection of sh-circ\_0002360 downregulated the circ\_0002360 level but had no significant expression change of RUNX1 in A549/DDP and H1299/DDP cells, relative to transfection of sh-NC (Figure 2a). IC50 of DDP was decreased in sh-circ\_0002360-transfected cells in contrast with sh-NC-transfected cells (Figure 2b). The results of colony formation assay (Figure 2c) and EdU staining assay (Figure 2d) demonstrated the inhibitory regulation of circ\_0002360 in cell proliferation ability. The migrated cells were significantly reduced in the sh-circ\_0002360 group compared with the sh-NC group (Figure 2e,f). The apoptosis rate by flow cytometry (Figure 2g) and caspase 3 activity by caspase 3 assay (Figure 2h) showed that circ\_0002360 inhibition accelerated cell apoptosis. The resistance proteins (MRP1 and P-gp) were inhibited and apoptosis protein (Bax) was upregulated, as indicated in the results of circ\_0002360 knockdown in A549/DDP and H1299/DDP cells (Figure 2i,j). Hence, DDP resistance and cell progression were impeded after downregulation of circ\_0002360.

## Circ\_0002360 positively regulated the level of ZNF300

ZNF300 mRNA expression was enhanced in lung cancer tissues relative to normal tissues (Figure 3a) and tumor-R

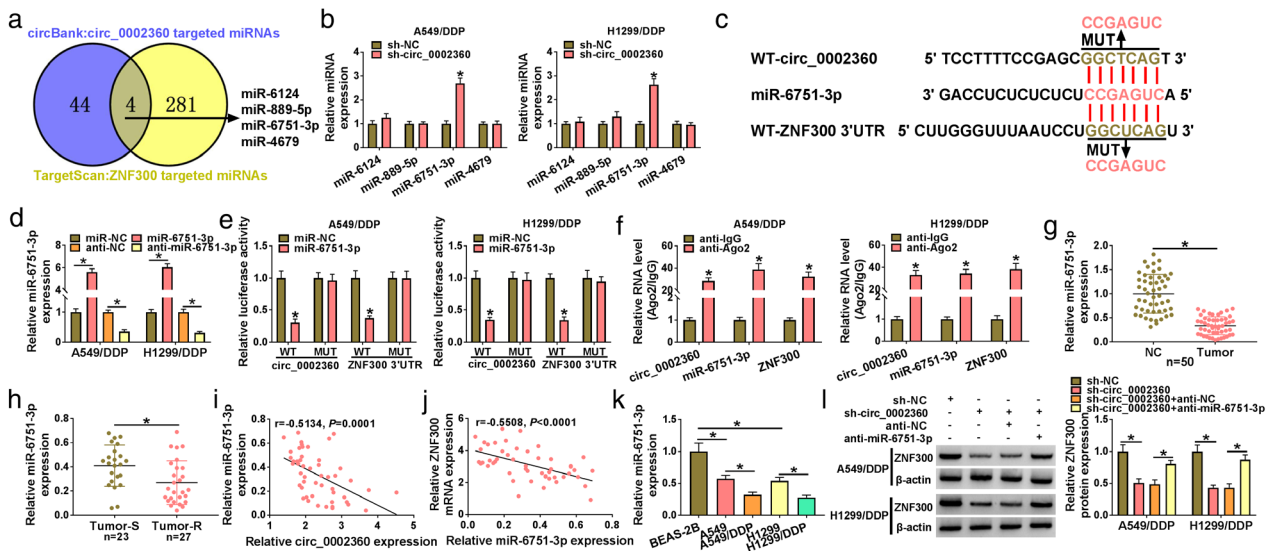


**FIGURE 6** Circ\_0002360 modulated ZNF300 level via targeting miR-6751-3p. (a) The miRNAs were screened through Venn diagram from circBank and Targetscan. (b) miR-6124, miR-889-5p, miR-6751-3p and miR-4679 levels were examined by RT-qPCR in sh-NC or sh-circ\_0002360-transfected A549/DDP and H1299/DDP cells. (c) The target binding sites between circ\_0002360 or ZNF300 and miR-6751-3p. (d) The efficiencies of miR-6751-3p and anti-miR-6751-3p were assessed via RT-qPCR. (e,f) Dual-luciferase reporter assay (e) and RIP assay (f) were performed to identify the interaction between circ\_0002360 or ZNF300 and miR-6751-3p. (g,h) RT-qPCR was used for miR-6751-3p quantification in lung cancer tissues (g) and tumor-R samples (h). (i,j) Pearson's correlation coefficient was used for linear analysis between miR-6751-3p and circ\_0002360 (i) and ZNF300 (j). (k) The miR-6751-3p level was examined using RT-qPCR in A549/DDP and H1299/DDP cells. (l) ZNF300 protein detection was performed through western blot after transfection of sh-NC, sh-circ\_0002360, sh-circ\_0002360 + anti-NC and sh-circ\_0002360 + anti-miR-6751-3p. \* $p < 0.05$

tissues relative to tumor-S tissues (Figure 3b). Pearson's correlation coefficient analysis showed that circ\_0002360 level was positively associated with ZNF300 mRNA level ( $r = 0.7563$ ,  $p < 0.0001$ ) in tumor-R samples (Figure 3c). The TCGA dataset showed that ZNF300 was highly expressed in lung adenocarcinoma (LUAD) and lung squamous cell carcinoma (LUSC) samples (Figure 3d). Also, the protein expression of ZNF300 was increased in the Tumor-R group (Figure 3e) and DDP-resistant lung cancer cells (Figure 3f), in contrast to the Tumor-S group and the parental lung cancer cells. ZNF300 was overexpressed by transfection of ZNF300 (relative to the vector group) in A549/DDP and H1299/DDP cells (Figure 3g). Knockdown of circ\_0002360 induced the obvious downregulation of ZNF300 protein level, which was eliminated by ZNF300 transfection in A549/DDP and H1299/DDP cells (Figure 3h). These results confirmed that circ\_0002360 resulted in the positive regulation of ZNF300.

## ZNF300 downregulation inhibited DDP resistance and lung cancer progression

The role of ZNF300 was then explored in DDP-resistant lung cancer cells. The protein level of ZNF300 was reduced in the sh-ZNF300 group in contrast with the sh-NC group (Figure 4a). After ZNF300 was downregulated, IC<sub>50</sub> of DDP (Figure 4b) and cell proliferation ability (Figure 4c,d) were shown to be repressed in A549/DDP and H1299/DDP cells. Silencing ZNF300 in A549/DDP and H1299/DDP cells induced the inhibition of migration capacity (Figure 4e) and acceleration of apoptosis (Figure 4g,h). MRP1 and P-gp protein levels were downregulated, while Bax protein expression was elevated in the sh-ZNF300 group, relative to the sh-NC group (Figure 4i,j). Taken together, ZNF300 promoted chemoresistance and oncogenesis in DDP-resistant lung cancer cells.

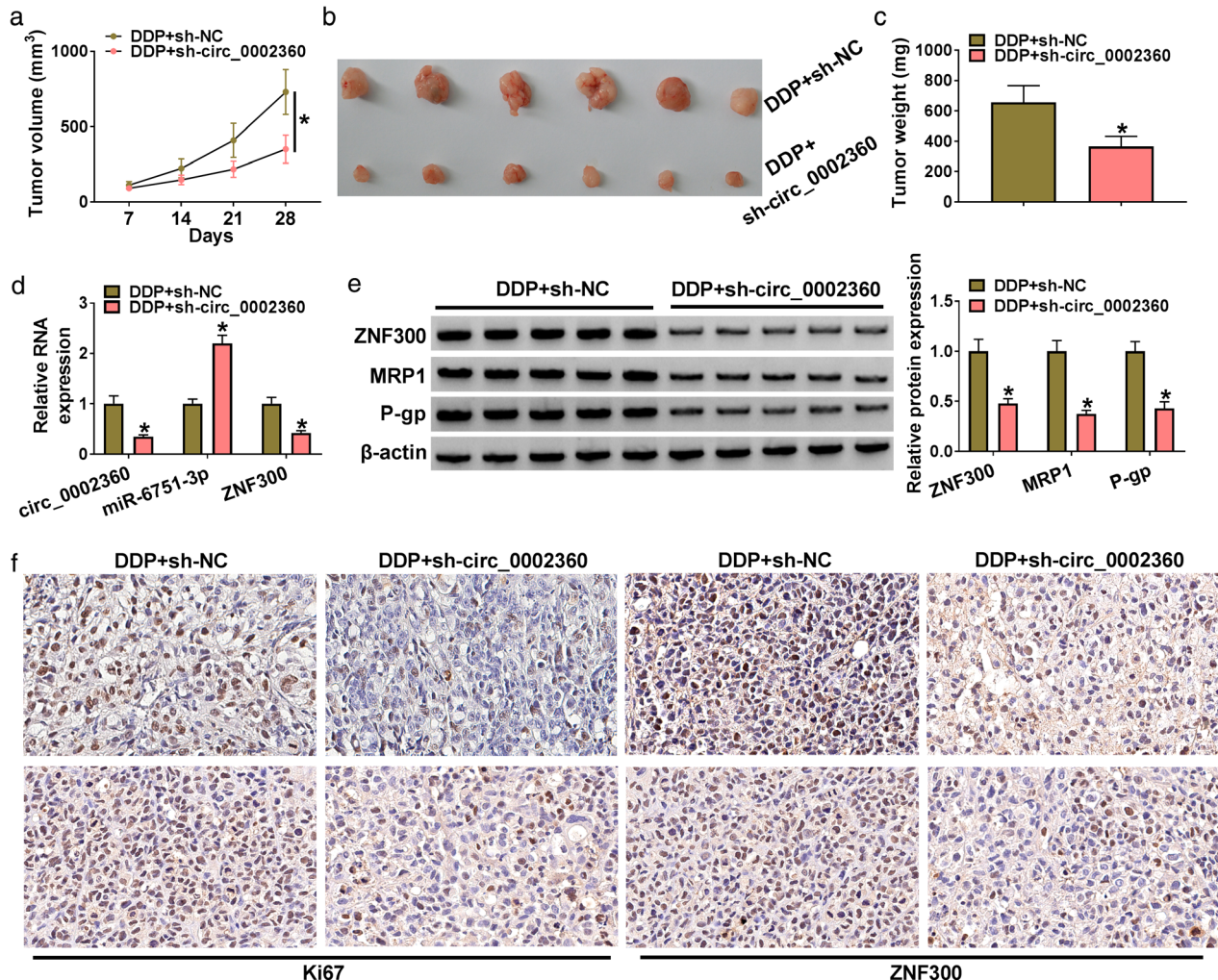


**FIGURE 7** Circ\_0002360 regulated DDP resistance in H1299/DDP xenograft mice via miR-6751-3p/ZNF300 axis. H1299/DDP xenograft model of the DDP + sh-NC or DDP + sh-circ\_0002360 group was established in mice. (a) Tumor volume was measured every 7 days. (b) Tumor images of each group. (c) Tumors were weighed. (d) circ\_0002360, miR-6751-3p and ZNF300 levels in tissues were determined using RT-qPCR. (e) ZNF300, MRP1 and p-gp protein levels were examined by western blot. (f) Ki67 and ZNF300 protein levels were analyzed via IHC assay. \* $p < 0.05$



## Circ\_0002360 acted in DDP-resistant lung cancer cells via upregulating ZNF300

Given the same function of circ\_0002360 and ZNF300 in regulating DDP resistance and cancer progression, we further studied whether circ\_0002360 function was related to ZNF300. A549/DDP and H1299/DDP cells were transfected with sh-circ\_0002360, sh-circ\_0002360 + ZNF300 and the control groups. The sh-circ\_0002360-induced inhibitory effects on IC<sub>50</sub> of DDP (Figure 5a), proliferation (Figure 5b,c) and migration (Figure 5d) were abrogated by transfection of ZNF300. Also, overexpression of ZNF300 attenuated the enhancement of apoptosis (Figure 5e,f) and changes of protein markers (MRP1, P-gp, Bax) (Figure 5g, h) caused by sh-circ\_0002360. Thus, the regulatory role of circ\_0002360 was partly attributed to the upregulation of ZNF300.

## Circ\_0002360 modulated ZNF300 level via targeting miR-6751-3p

Circbank and Targetscan were used to search the target miRNAs by circ\_0002360 and ZNF300. As shown in Figure 6a, there were four miRNAs (miR-6124, miR-889-5p, miR-6751-3p, miR-4679) predicted by the software. Only miR-6751-3p was significantly upregulated by knockdown of circ\_0002360 in A549/DDP and H1299/DDP cells (Figure 6b). Then, miR-6751-3p was selected for target research. The binding sites between circ\_0002360 or ZNF300 and miR-6751-3p are shown in Figure 6c. The efficiencies of miR-6751-3p and anti-miR-6751-3p transfection were evident in A549/DDP and H1299/DDP cells (Figure 6d). The luciferase activities of WT-circ\_0002360 and WT-ZNF300 3'UTR groups were suppressed by miR-6751-3p upregulation, while no effect was detected in the MUT-circ\_0002360 and MUT-ZNF300 3'UTR

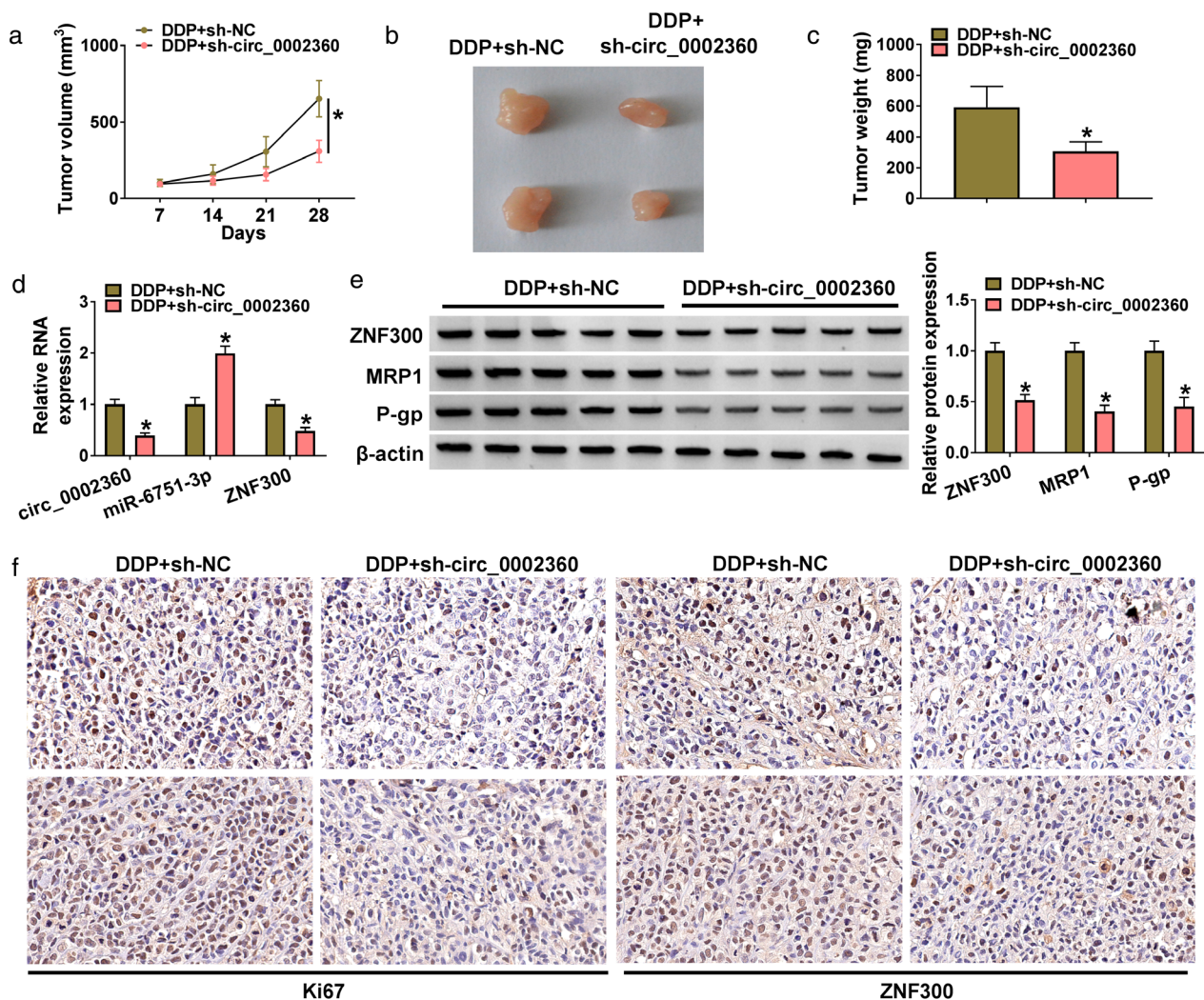


**FIGURE 8** Circ\_0002360 regulated DDP resistance in A549/DDP xenograft mice by miR-6751-3p/ZNF300 axis. A549/DDP xenograft model of the DDP + sh-NC or DDP + sh-circ\_0002360 group was established in mice. (a–c) Tumor volume (a) and weight (b,c) were measured. (d) Circ\_0002360, miR-6751-3p and ZNF300 levels in tissues were examined by RT-qPCR. (e) ZNF300, MRP1 and p-gp protein detection was performed by western blot. (f) IHC assay was used for protein analysis of Ki67 and ZNF300 in tumor tissues. \* $p < 0.05$

groups (Figure 6e). The levels of circ\_0002360, miR-6751-3p and ZNF300 were higher in the anti-Ago2 group than those in the anti-IgG group (Figure 6f). Hence, circ\_0002360 or ZNF300 could interact with miR-6751-3p. The miR-6751-3p expression was downregulated in lung cancer tissues relative to normal tissues (Figure 6g), and significant downregulation was found in tumor-R samples compared with tumor-S samples (Figure 6h). Linear analysis demonstrated that circ\_0002360 had a negative relationship ( $r = -0.5134$ ,  $p = 0.0001$ ) with miR-6751-3p (Figure 6i) and miR-6751-3p was also negatively related to ZNF300 ( $r = -0.5508$ ,  $p < 0.0001$ ) (Figure 6j). In comparison with A549 and H1299 cells, miR-6751-3p level was reduced in A549/DDP and H1299/DDP cells (Figure 6k). Moreover, anti-miR-6751-3p transfection relieved the sh-circ\_0002360-mediated protein expression inhibition of ZNF300 in A549/DDP and H1299/DDP cells (Figure 6l). These results suggested that circ\_0002360 targeted miR-6751-3p to affect the ZNF300 level.

### Circ\_0002360 regulated DDP resistance in xenograft mice the miR-6751-3p/ZNF300 axis

The effect of DDP on tumor growth and drug resistance of DDP-resistant cells was assessed in mice models. The results indicated that DDP significantly inhibited tumor volume and weight of H1299 and A549 xenograft models, and DDP-induced tumor growth inhibition was attenuated in H1299/DDP and A549/DDP models due to drug resistance (Figure S1). The influence of circ\_0002360 on DDP resistance in vivo was then studied further. Tumor volume (Figure 7a) and weight (Figure 7b,c) were inhibited in the DDP + sh-circ\_0002360 group in contrast with the DDP + sh-NC group, showing that circ\_0002360 knockdown enhanced DDP sensitivity in mice. RT-qPCR showed that circ\_0002360 and ZNF300 levels were downregulated but miR-6751-3p was upregulated in tumor tissues of the DDP + sh-circ\_0002360 group relative to the DDP + sh-NC group (Figure 7d). The protein detection by western blot manifested that circ\_0002360 inhibition resulted in the expression reduction of ZNF300, MRP1, P-gp (Figure 7e). Also, the IHC assay suggested that Ki67 and ZNF300 protein levels were downregulated in the DDP + sh-circ\_0002360 group compared with the DDP + sh-NC group (Figure 7f). Meanwhile, the xenograft model of A549/DDP cells showed that sh-circ\_0002360 reduced DDP resistance in mice by affecting miR-6751 and ZNF300 levels (Figure 8). Overall, silencing circ\_0002360 repressed DDP resistance by targeting the miR-6751-3p/ZNF300 axis in vivo.

## DISCUSSION

The emergence of chemoresistance has resulted in adverse impacts on therapeutic outcomes of cancers.<sup>18</sup> In this study, we found that circ\_0002360 knockdown could suppress

drug resistance and malignant development via acting on the miR-6751-3p/ZNF300 molecular pathway in DDP-resistant lung cancer cells.

CircRNAs are functional molecules which are involved in a variety of biological behaviors, such as tumor occurrence, metastasis, and chemoresistance.<sup>19</sup> The expression reduction of circFoxo3 has been reported to improve cell survival, migration and docetaxel resistance in prostate cancer.<sup>20</sup> CircAMOTL1 exerted an important effect on paclitaxel resistance of breast cancer cells,<sup>21</sup> and circ-FBXW7 attenuated the resistance against oxaliplatin in colorectal cancer.<sup>22</sup> DDP is one of the most frequently used therapeutic agents in human cancers.<sup>23</sup> In this study, circ\_0002360 level was higher in resistant samples and cells compared to sensitive controls. Furthermore, cellular experiments demonstrated that silencing circ\_0002360 repressed DDP resistance, cell growth and migration while accelerated cell apoptosis. Circ\_0002360 was related to DDP resistance and lung cancer progression, and circ\_0002360 level inhibition could enhance sensitivity of DDP.

ZNF300 plays a pivotal role in the embryonic development of mammals. Wang et al. discovered that ZNF300 upregulation contributed to the growth and metastasis of cervical cancer cells in vitro.<sup>24</sup> Yu et al. reported that ZNF300 increased chemoresistance of non-small cell lung cancer (NSCLC) cells to DDP.<sup>13</sup> In accordance with this report, our data confirmed that downregulation of ZNF300 restrained DDP resistance and progressive cell behaviors. Thus, ZNF300 is an important gene in generating DDP resistance of lung cancer.

Interestingly, circ\_0002360 could regulate the level of ZNF300 in a positive way and overexpression of ZNF300 partly abolished the resistance inhibition induced by silence of circ\_0002360. The functions of circ\_0002360 in chemoresistance and carcinogenesis were correlated with the expression change of ZNF300 in lung cancer. CircRNAs are known to serve as miRNA inhibitors to mediate gene levels in biological regulation of lung cancer.<sup>25</sup> Circ\_0001361 has been found to be dependent on the miR-525-5p/VMA21 axis to promote tumorigenesis and progression of lung adenocarcinoma.<sup>26</sup> Interfering circ\_00014130 reduced chemoresistance and malignance in docetaxel-resistant NSCLC cells through interacting with the miR-545-3p/YAP1 network.<sup>27</sup> Additionally, circRNA\_103809/miR-377-3p/GOT1 axis affected chemosensitivity of DDP in lung cancer cells.<sup>10</sup> This study identified miR-6751-3p as a possible miRNA between circ\_0002360 and ZNF300. As expected, circ\_0002360 or ZNF300 could combine with miR-6751-3p and ZNF300 level was increased by circ\_0002360/miR-6751-3p interaction axis. Given that circ\_0002360 functioned in DDP-resistant cell lines by increasing ZNF300 level, circ\_0002360/miR-6751-3p/ZNF300 was considered to be implicated in DDP resistance and tumor development in lung cancer.

An in vivo assay also showed that circ\_0002360 regulated DDP susceptibility and tumor growth in mice through modulating the miR-6751-3p and ZNF300 levels. However,

the reverted experiments of miR-6751-3p and ZNF300 for circ\_0002360 remain to be performed in a future study. It is necessary to support the conclusion that circ\_0002360 mediated DDP resistance in lung cancer via the miR-6751-3p/ZNF300 axis.

In conclusion, circ\_0002360 downregulation inhibited chemoresistance and oncogenesis of DDP-resistant lung cancer through targeting miR-6751-3p/ZNF300 axis. The current study provides first-hand information for circ\_0002360 function and circ\_0002360/miR-6751-3p/ZNF300 axis in regulating DDP resistance of lung cancer, thus contributing to understanding the molecular mechanism of chemoresistance in lung cancer.

## CONFLICT OF INTEREST

The authors declare that they have no conflicts of interest.

## ORCID

Zhaohui Tang  <https://orcid.org/0000-0002-0721-8657>

## REFERENCES

1. Thai AA, Solomon BJ, Sequist LV, Gainor JF, Heist RS. Lung cancer. *Lancet*. 2021;398:535–54.
2. El-Hussein A, Manoto SL, Ombinda-Lemboumba S, Alrowaili ZA, Mthunzi-Kufa P. A review of chemotherapy and photodynamic therapy for lung cancer treatment. *Anticancer Agents Med Chem*. 2021; 21:149–61.
3. Arbour KC, Riely GJ. Systemic therapy for locally advanced and metastatic non-small cell lung cancer: a review. *JAMA*. 2019;322:764–74.
4. He G, Xiao X, Zou M, Zhang C, Xia S. Pemetrexed/cisplatin as first-line chemotherapy for advanced lung cancer with brain metastases: a case report and literature review. *Medicine (Baltimore)*. 2016;95: e4401.
5. Wang Y, Wang Y, Qin Z, Cai S, Yu L, Hu H, et al. The role of non-coding RNAs in ABC transporters regulation and their clinical implications of multidrug resistance in cancer. *Expert Opin Drug Metab Toxicol*. 2021;17:291–306.
6. Zhang M, Bai X, Zeng X, Liu J, Liu F, Zhang Z. circRNA-miRNA-mRNA in breast cancer. *Clin Chim Acta*. 2021;523:120–30.
7. Ameli-Mojarad M, Ameli-Mojarad M, Hadizadeh M, Young C, Babini H, Nazemalhosseini-Mojarad E, et al. The effective function of circular RNA in colorectal cancer. *Cancer Cell Int*. 2021;21:496.
8. Lan H, Yuan J, Zeng D, Liu C, Guo X, Yong J, et al. The emerging role of non-coding RNAs in drug resistance of ovarian cancer. *Front Genet*. 2021;12:693259.
9. Xu J, Ni L, Zhao F, Dai X, Tao J, Pan J, et al. Overexpression of hsa\_circ\_0002874 promotes resistance of non-small cell lung cancer to paclitaxel by modulating miR-1273f/MDM2/p53 pathway. *Aging (Albany NY)*. 2021;13:5986–6009.
10. Zhu X, Han J, Lan H, Lin Q, Wang Y, Sun X. A novel circular RNA hsa\_circRNA\_103809/miR-377-3p/GOT1 pathway regulates cisplatin-resistance in non-small cell lung cancer (NSCLC). *BMC Cancer*. 2020; 20:1190.
11. Chen Z, Jie Y, Qiu Z, Zhang M, Shi B, Zhu X, et al. Expression profile and bioinformatics analysis of circular RNAs in tongue squamous cell carcinoma. *Oral Dis*. 2021. Online ahead of print.
12. Yan Y, Zhang R, Zhang X, Zhang A, Zhang Y, Bu X. RNA-Seq profiling of circular RNAs and potential function of hsa\_circ\_0002360 in human lung adenocarcinoma. *Am J Transl Res*. 2019;11:160–75.
13. Yu S, Ao Z, Wu Y, Song L, Zhang P, Li X, et al. ZNF300 promotes chemoresistance and aggressive behaviour in non-small-cell lung cancer. *Cell Prolif*. 2020;53:e12924.
14. Wang R, Ma X, Su S, Liu Y. Triptolide antagonized the cisplatin resistance in human ovarian cancer cell line A2780/CP70 via hsa-mir-6751. *Future Med Chem*. 2018;10:1947–55.
15. Livak KJ, Schmittgen TD. Analysis of relative gene expression data using real-time quantitative PCR and the 2(-Delta Delta C(T)) method. *Methods*. 2001;25:402–8.
16. Zhou D, Lin X, Wang P, Yang Y, Zheng J, Zhou D. Circular RNA circ\_0001162 promotes cell proliferation and invasion of glioma via the miR-936/ERBB4 axis. *Bioengineered*. 2021;12:2106–18.
17. Sun J, Xin K, Leng C, Ge J. Down-regulation of SNHG16 alleviates the acute lung injury in sepsis rats through miR-128-3p/HMGB3 axis. *BMC Pulm Med*. 2021;21:191.
18. Li GH, Qu Q, Qi TT, Teng XQ, Zhu HH, Wang JJ, et al. Super-enhancers: a new frontier for epigenetic modifiers in cancer chemoresistance. *J Exp Clin Cancer Res*. 2021;40:174.
19. Cheng XY, Shen H. Circular RNA in lung cancer research: biogenesis, functions and roles. *Zhongguo Fei Ai Za Zhi*. 2018;21:50–6.
20. Shen Z, Zhou L, Zhang C, Xu J. Reduction of circular RNA Foxo3 promotes prostate cancer progression and chemoresistance to docetaxel. *Cancer Lett*. 2020;468:88–101.
21. Ma J, Fang L, Yang Q, Hibberd S, du WW, Wu N, et al. Posttranscriptional regulation of AKT by circular RNA angiomin-1 like 1 mediates chemoresistance against paclitaxel in breast cancer cells. *Aging (Albany NY)*. 2019;11:11369–81.
22. Xu Y, Qiu A, Peng F, Tan X, Wang J, Gong X. Exosomal transfer of circular RNA FBXW7 ameliorates the chemoresistance to oxaliplatin in colorectal cancer by sponging miR-18b-5p. *Neoplasma*. 2021;68: 108–18.
23. Makovec T. Cisplatin and beyond: molecular mechanisms of action and drug resistance development in cancer chemotherapy. *Radiol Oncol*. 2019;53:148–58.
24. Wang T, Wang XG, Xu JH, Wu XP, Qiu HL, Yi H, et al. Over-expression of the human ZNF300 gene enhances growth and metastasis of cancer cells through activating NF- $\kappa$ B pathway. *J Cell Mol Med*. 2012;16:1134–45.
25. Dong H, Zhou J, Cheng Y, Wang M, Wang S, Xu H. Biogenesis, functions, and role of CircRNAs in lung cancer. *Cancer Manag Res*. 2021; 13:6651–71.
26. Shen HY, Shi LX, Wang L, Fang LP, Xu W, Xu JQ, et al. Hsa\_circ\_0001361 facilitates the progress of lung adenocarcinoma cells via targeting miR-525-5p/VMA21 axis. *J Transl Med*. 2021;19:389.
27. Du D, Cao X, Duan X, Zhang X. Blocking circ\_0014130 suppressed drug resistance and malignant behaviors of docetaxel resistance-acquired NSCLC cells via regulating miR-545-3p-YAP1 axis. *Cyto-technology*. 2021;73:571–84.

## SUPPORTING INFORMATION

Additional supporting information may be found in the online version of the article at the publisher's website.

**How to cite this article:** Ding L, Li L, Tang Z. Cisplatin resistance and malignant behaviors of lung cancer cells are promoted by circ\_0002360 via targeting miR-6751-3p to regulate the expression of ZNF300. *Thorac Cancer*. 2022;13:986–96. <https://doi.org/10.1111/1759-7714.14342>